

Quantum phases of frustrated 2-leg spin-1/2 ladders with skewed rungs

Geetanjali Giri,^{1,*} Dayasindhu Dey,^{2,†} Manoranjan Kumar,^{2,‡} S. Ramasesha,^{1,§} and Zoltán G. Soos^{3,¶}

¹*Solid State and Structural Chemistry Unit, Indian Institute of Science, Bangalore 560012, India*

²*S. N. Bose National Centre for Basic Sciences,
Block - JD, Sector - III, Salt Lake, Kolkata - 700098, India*

³*Department of Chemistry, Princeton University, Princeton, New Jersey 08544, USA*

(Dated: March 7, 2024)

The quantum phases of 2-leg spin-1/2 ladders with skewed rungs are obtained using exact diagonalization of systems with up to 26 spins and by density matrix renormalization group calculations to 500 spins. The ladders have isotropic antiferromagnetic (AF) exchange $J_2 > 0$ between first neighbors in the legs, variable isotropic AF exchange J_1 between some first neighbors in different legs, and an unpaired spin per odd-membered ring when $J_1 \gg J_2$. Ladders with skewed rungs and variable J_1 have frustrated AF interactions leading to multiple quantum phases: AF at small J_1 , either F or AF at large J_1 , as well as bond-order-wave phases or reentrant AF (singlet) phases at intermediate J_1 .

PACS numbers: 77.55.Nv, 77.84.Jd, 75.50.Xx

I. INTRODUCTION

Many different kinds of spin chains have been studied over years. Bethe¹ and Hulthén² obtained the ground state (GS) of the linear spin-1/2 Heisenberg antiferromagnet (HAF). The HAF is a prototypical gapless system with isotropic exchange $J > 0$ between neighbors and is closely realized in crystals that contain $S = 1/2$ transition metal ions or organic molecular ions. Haldane³ pointed out that the spin-1 HAF is a gapped system as was soon confirmed both experimentally and numerically. The J_1 - J_2 model, Eq. 1 below, has isotropic J_1 , J_2 between first and second neighbors, respectively. It has been extensively studied in connection with frustrated interactions.⁴⁻⁹ Depending on the ratio J_1/J_2 , the system has gapless phases with quasi-long-range order and gapped dimer or incommensurate phases.¹⁰ Even when limited to spin-1/2 chains, there is considerable freedom in the number and range of exchange interactions, in the choice of isotropic (Heisenberg), anisotropic or antisymmetric exchange, or spin ladders with two or more parallel chains. Sandvik¹¹ has reviewed numerical approaches to spin chains and ladders.

There is considerable interest in the spin gap of the fermionic chains for applications in singlet fission.^{12,13} The spin gap can be reduced by raising the energy of the GS with respect to the triplet state, by introducing kinetic frustration, via fused odd membered rings. Thomas et al.¹⁴ studied the fused azulenes both in spin models with isotropic antiferromagnetic exchange interaction and in the Pariser-Parr-Pople (PPP) model for π -electrons. The azulene molecule ($C_{10}H_8$) has fused 5 and 7 membered rings that, when fused into a polymer, define the unit cell of a 2-leg ladder with skewed rungs. To their surprise Thomas et al.¹⁴ found that the spin of the GS of the system increased with system size in both models.

Recent interest in spin chains has focused on exotic quantum phases^{8,9} and the possibility of multiferroic ma-

terials.¹⁴⁻¹⁸ However, so far there has not been a systematic study to improve the rate at which the GS spin increases or to unravel the reason behind cascading spin of the GS with increasing system size. This study is aimed at understanding the magnetic GS of fused azulene in particular and fused frustrated ring systems in general.

We obtain in this paper the quantum phases of frustrated 2-leg spin-1/2 ladders with skewed rungs. Such ladders have not been studied previously to the best of our knowledge. The ladders can be viewed as generalizations of the J_1 - J_2 model: Isotropic J_2 between second neighbors corresponds to HAFs on legs of odd and even numbered sites; isotropic J_1 between first neighbors corresponds to two zig-zag rungs per site. The ladders we discuss have fewer J_1 rungs as illustrated in Fig. 1. The rungs of the 5/7 ladder correspond to fused azulenes while the rungs of the 3/4 ladder define alternating fused 3 and 4-membered rings. We consider ladders with variable number of spins, variable $J_1 > 0$ and constant $J_2 = 1$. Ladders with skewed rungs may have equivalent legs (Fig. 1b) or inequivalent legs (Fig. 1a) in addition to at least one frustrated odd-membered ring per unit cell.

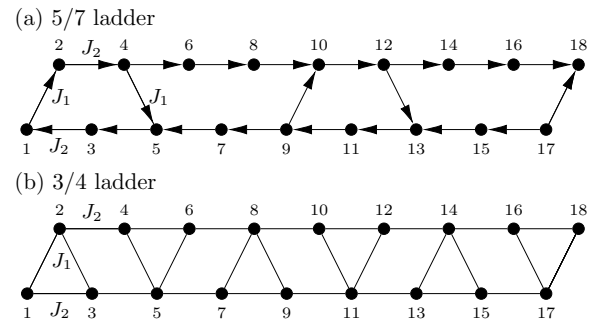


FIG. 1. Schematic representation of the 5/7 ladder (top) and 3/4 ladder (bottom) with isotropic exchange J_1 in rungs and J_2 between neighbors in legs. The arrows are discussed in Sec. V.

The legs of all ladders are conveniently numbered in Fig. 1 as odd or even integers. Each leg is a HAF with isotropic J_2 between neighbors and either periodic boundary conditions (PBC) or open boundary conditions (OBC). Skewed rungs with isotropic J_1 connect adjacent spins in this numbering. The J_1 - J_2 model is the 3/3 ladder

$$H_{3/3} = J_1 \sum_r \vec{S}_r \cdot \vec{S}_{r+1} + J_2 \sum_r \vec{S}_r \cdot \vec{S}_{r+2} \quad (1)$$

The 3/3 ladder has one spin per unit cell and the largest possible number of skewed rungs. The GS is a singlet, $S_G = 0$, in the entire sector $J_1, J_2 > 0$ that includes spin liquid phase and gapped dimer or incommensurate phases.¹⁰ All ladders in this paper have identical legs with $J_2 = 1$ in Eq. 1 and different numbers of J_1 rungs. The conventional 2-leg ladder is $H_{4/4}$ with one J_1 rung, two spins per unit cell, and inversion symmetry at the middle of every rung. The GS is a singlet^{19,20} with a finite singlet-triplet gap for $J_1 > 0$. Ladders with skewed rungs instead have inversion symmetry at some sites in one or both legs.

Quite generally, large $J_1 > J_2$ localizes a spin on every odd-membered ring. The sign of the effective exchange between spins determines whether the GS is ultimately F or AF in the thermodynamic limit. The total spin S is conserved and ranges from $S_G(J_1, N) = 0$ in AF ladders to $S_G(J_1, N) \propto N$ in F ladders with exchange $J_1 > J_2 = 1$. Increasing J_1 generates a variety of quantum phases. In addition to F or AF (singlet) phases, some ladders support bond order waves (BOWs) or reentrant AF phases as a function of $J_1/J_2 > 0$.

The present study was motivated by the 5/7 ladder in Fig. 1a. The GS is a singlet at $J_1 = 1$ for $N < 50$ and $S_G(1, N)$ increases slowly with system size.¹⁴ The origin of F interactions in systems with purely AF exchange and the thermodynamic limit are difficult to assess for the large unit cell of eight spins. We address both issues in ladders with smaller unit cells. It turns out that the evolution of $S_G(J_1, N)$ with J_1 or system size is quite variable in ladders with skewed rungs and leads to multiple quantum phases. The ladders share a common qualitative feature, however: The GS is always a singlet at small J_1 and changes of $S_G(J_1, N)$ typically cluster around $J_1 \sim 2$. In the approximation of singlet pairing of adjacent sites, or Kekulé valence bond diagrams, three J_2 bonds at small J_1 are converted into two J_1 bonds and two unpaired spins at large J_1 . Accurate treatment of ladders generates other phases at intermediate J_1 before reaching an AF or F phase at large J_1 .

The paper is organized as follows. Numerical methods are summarized in Sec. II. The quantum phases of the 3/4 and 5/5 ladders are presented in Sec. III. The 3/4 ladder has a first-order AF to F transition around $J_{1c} = 1.58$ while the 5/5 ladder has a narrow BOW phase and a singlet GS over the entire range. The 3/5 ladder in Sec. IV has multiple quantum phases at intermediate $J_1 \sim 2$ and frustrated effective exchanges leading to a singlet GS at

large J_1 . The 5/7 ladder in Sec. V also has multiple quantum phases at intermediate J_1 , including a reentrant AF phase, and a F phase for $J_1 > 2.4$ with an unpaired spin per rung. The discussion in Sec. VI summarizes the pattern of F or AF phases of other 2-leg ladders with skewed rungs.

II. NUMERICAL METHODS

We use exact diagonalization (ED) for ladders up to 26 spins. The relevant 24-spin ladders with PBC have an integral number of unit cells and sectors with inversion symmetry σ at some sites. The extra rung gives 26 spins in OBC ladders. Matrix elements, correlation functions and excited states are also computed.

We use the Density Matrix Renormalization Group (DMRG) technique²¹ to obtain the low energy states of larger OBC systems. The DMRG scheme for building skewed ladders is similar to building regular ladders and proceeds by adding two new sites at a time, starting with a ring of four sites. The schematic for building a 5/7 ladder is shown in Fig. 2. Since OBC ladders are asymmetric about the middle in general, we have used asymmetric DMRG in which we keep track of the left and right systems separately and have carried out 10 sweeps of the finite system DMRG. In the worst case, the truncation error in our calculation is below 10^{-11} by keeping up to $m = 500$ eigenvectors corresponding to the highest eigenvalues of the density matrix. The error in total energies are estimated to be less than $10^{-5}\%$ which leads to uncertainty in energy gaps of less than 10^{-4} . Comparable DMRG accuracy is discussed elsewhere for other kinds of spin chains.^{4,22-25} The largest ladders studied in this paper have almost 500 sites.

The total spin S is always conserved and is explicitly

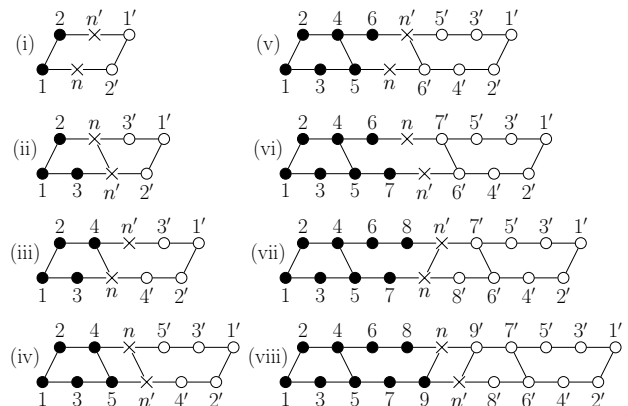


FIG. 2. Schematics of the DMRG steps to grow a 5/7 ladder. The filled (open) circles are the left (right) of the ladder and the crosses are the new sites introduced at each steps. While the left (right) is treated as the system the right (left) works as the environment. Other skewed ladders in this study are also similarly constructed.

taken into account in the valence bond (VB) basis,^{26,27} as is inversion symmetry at sites in PBC ladders. The spin $S_G(J_1, N)$ of the absolute GS is obtained by comparing the lowest energy in sectors with different S

$$\Gamma_S(N) = E_0(S, N) - E_0(0, N). \quad (2)$$

We have $S_G = 0$ when $\Gamma_S > 0$, level crossing when $\Gamma_S = 0$, and $S_G > 0$ given by the largest S_G for which $\Gamma_S < 0$. Similarly, the gap Γ_σ at fixed S_G is to the lowest state with reversed inversion symmetry

$$\Gamma_\sigma = E_0(S_G, \sigma = -1, N) - E_0(S_G, \sigma = 1, N). \quad (3)$$

The GS is even when $\Gamma_\sigma > 0$, odd when $\Gamma_\sigma < 0$, and doubly degenerate when $\Gamma_\sigma = 0$. The singlet-triplet gap $\Gamma_T(N)$ is the excitation energy to the lowest triplet state in systems whose GS is a singlet, $S_G = 0$.

DMRG gives accurate results for the low-energy states of long ladders. The z component of the total spin, S^z , is conserved and exploiting this conservation is straightforward. The highest S^z value for which $E_0(S^z) - E_0(0)$ is zero defines the spin S_G of the GS. $S_G(J_1, N)$ is inferred from the energies of the lowest S^z states. When $S_G > 0$, the $(2S_G + 1)$ Zeeman components are degenerate. Hence $E_0(0, N)$ is an excited state in the $S^z = 0$ sector, as are the $S^z = 0$ components of states with $S < S_G$. It follows that DMRG gives $E_0(S^z, N) - E_0(S^z - 1, N) = 0$ when S_G increases from $S_G - 1$ to S_G . In practice, we start with $S^z = 0$ and increase it by integer steps; S_G is reached when the E_0 at $S^z = S_G + 1$ is higher than at $S^z = S_G$.¹⁴ Although DMRG does not specify inversion symmetry, the GS is degenerate within the numerical accuracy when $\Gamma_\sigma(N) = 0$.

III. THE 3/4 AND 5/5 LADDERS

The 3/4 ladder in Fig. 1b has 2/3 as many J_1 rungs as the J_1 - J_2 ladder. It has two consecutive J_1 followed by a missing rung. The Hamiltonian is

$$H_{3/4} = J_1 \sum_r \vec{S}_{3r-1} \cdot (\vec{S}_{3r-2} + \vec{S}_{3r}) + J_2 \sum_r \vec{S}_r \cdot \vec{S}_{r+2}. \quad (4)$$

The PBC ladder has three spins per unit cell and inversion symmetry at the apex of isosceles triangles with sides J_1 and base J_2 . As shown in Fig. 3, the PBC ladder of $N = 8n = 24$ spins has a singlet GS for $J_1 < J_{1c}(N)$ and $S_G = 4n/3$ for $J_1 > J_{1c}$. Each triangle has an unpaired spin and the jump from $S_G = 0$ to 4 at $J_{1c} = 1.58$ indicates a ferromagnetic effective exchange between triangles. The inset shows J_2 exchanges at sites 2,4 and 3,5 of adjacent triangles.

In addition to the spin S_G as a function of $J_1 \geq 0$, $J_2 = 1$, we compute the spin density ρ_j at site j and spin correlation functions $C(j, k)$ as the expectation values

$$\begin{aligned} \rho_j &= 2\langle G | S_j^z | G \rangle \\ C(j, k) &= \langle G | \vec{S}_j \cdot \vec{S}_k | G \rangle. \end{aligned} \quad (5)$$

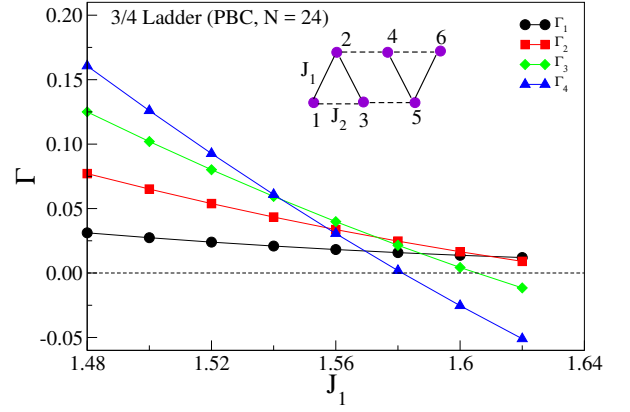


FIG. 3. Energy differences Γ_S in Eq. 2 in sectors with total spin S as a function of J_1 for a 3/4 ladder with PBC and 24 spins; inset: two unit cells of the 3/4 ladder under PBC.

TABLE I. First and second neighbor spin correlation functions $C(j, k)$ of the 3/4 ladder with PBC and $N = 24$ spins. Refer to Fig. 1 for site numbers.

J_1	$C(1, 2), C(2, 3)$	$C(3, 4)$	$C(1, 3)$	$C(2, 4), C(3, 5)$
0	0	0	-0.4489	-0.4489
1	-0.1201	0.0972	-0.3587	-0.4255
1.5	-0.3004	0.1801	-0.0363	-0.3522
1.56	-0.3215	0.1975	0.0036	-0.3400
2	-0.4480	0.2272	0.2350	-0.2497
5	-0.4923	0.1655	0.2486	-0.1308
20	-0.4995	0.1253	0.2499	-0.0737
40	-0.4999	0.1182	0.2500	-0.0646

Spin densities vanish identically in singlet states. The PBC ladder has two first-neighbor spin correlations in Table I with $k = j \pm 1$ that vanish at $J_1 = 0$ and two second-neighbor correlations with $k = j \pm 2$, one of which changes sign with increasing J_1 .

Spins in different legs are uncorrelated at $J_1 = 0$. The second neighbor correlations at $J_1 = 0$ are $(1/4 - \ln 2) = -0.44315$ in the thermodynamic limit. Finite size effects are fairly small at $N = 24$. The sign of $C(1, 3)$ changes near the jump from $S_G = 0$ to 4. The triangles at large J_1 have a doublet GS with $C(1, 2) = C(2, 3) = -0.5$ and $C(1, 3) = 0.25$ that are almost reached at $J_1 = 5$. The limiting spin densities are $\rho_a = -1/3$ at the apex and $\rho_b = 2/3$ at each base, which gives an unpaired spin per triangle. The spin densities at $J_1 = 5$ and 20 are, respectively, $\rho_a = -0.4269$ and -0.3578 , and $\rho_b = 0.7135$ and 0.6789 . They converge more slowly with J_1 than spin correlations. At large J_1 we have $C(2, 4) = C(3, 5) = \rho_a \rho_b / 4 = -1/18 = -0.0556$. The limit now requires $J_1 > 40$ due to the slow evolution of spin densities.

The OBC ladders have $N = 8n + 2$ spins and a J_1 rung between sites $8n + 1$ and $8n + 2$. The GS still has $S_G = 4n/3$ and one unpaired spin per triangle for $J_1 \geq 1.6$. DMRG results in Fig. 4, upper panel, have increasing S_G and indicate a F phase in the thermodynamic limit with

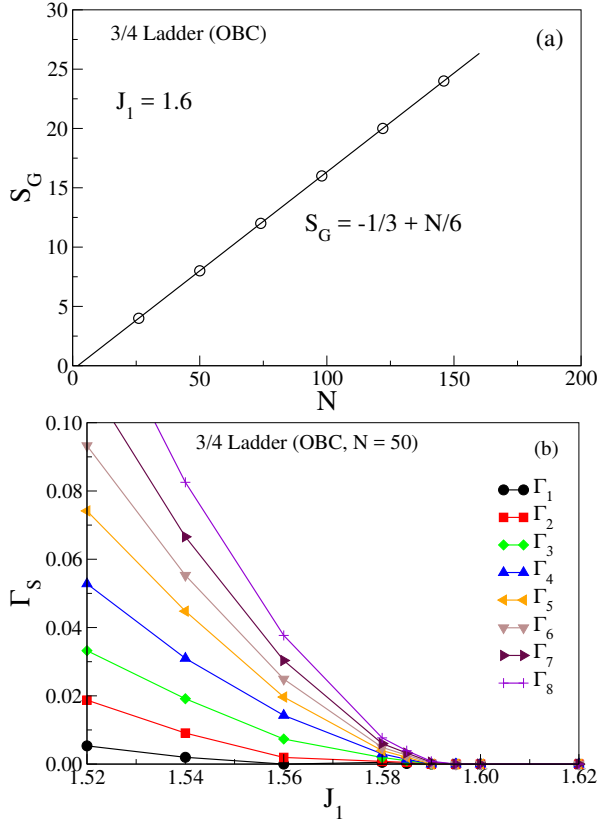


FIG. 4. (a) The GS spin S_G of 3/4 ladders with OBC and $J_1 = 1.6$ as a function of system size. The F phase has one spin per triangle. (b) The energy difference Γ_S between the GS in sectors with $S^z = S_G$ to 0 as a function of J_1 for a 3/4 ladder with OBC and 50 spins.

one spin per three-membered ring. S_G changes rapidly but sequentially with increasing J_1 in OBC ladders, from $S_G = 0$ to 4 for 24 spins. DMRG for 50 spins in Fig. 4, lower panel, shows that S_G jumps from 0 to 1 at $J_1 = 1.56$ and reaches the expected $S_G = 8$ by $J_1 = 1.59$.

The ferromagnetism of 3/4 ladders for $J_1 > 1.58$ is an example of the McConnell mechanism²⁸ with AF exchange (here J_2) between sites with positive and negative spin densities to obtain a F interaction. The effective F exchange between adjacent triangles is $J_{\text{eff}} = 2J_2\rho_a\rho_b$ and goes to $-4/9$ for $J_2 = 1$ in the limit $J_1 \gg 1$. The McConnell idea has been generalized to inorganic as well as organic radicals²⁹ with delocalized electrons and has been realized experimentally at low temperature in oligomers of spin-1/2 radicals.³⁰

The 5/5 ladder (Fig. 5, inset) has two exchanges J_1 per six J_2 . The Hamiltonian is

$$H_{5/5} = J_1 \sum_r \vec{S}_{3r-2} \cdot \vec{S}_{3r-1} + J_2 \sum_r \vec{S}_r \cdot \vec{S}_{r+2}. \quad (6)$$

There are half as many rungs as in the 3/4 ladder. The GS is a singlet, $S_G = 0$, over the entire range $J_1 > 0$. Large J_1 localizes a spin at sites $3r$, the only sites without a J_1 rung. Second order perturbation theory gives an AF

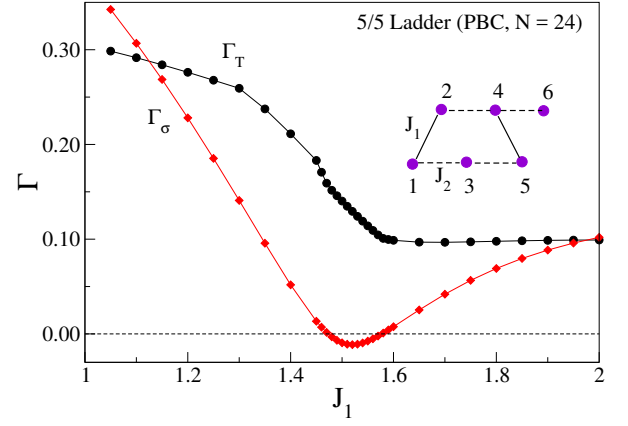


FIG. 5. Excitation energies of a 5/5 ladder with PBC and 24 spins: Γ_T to the lowest triplet state and Γ_σ to the lowest singlet with opposite inversion symmetry to the singlet GS; inset: two unit cells.

TABLE II. Spin correlation functions $C(j, k)$ at sites $3r$ of the 5/5 ladder with PBC and $N = 24$. Refer to Fig. 5, inset, for site numbers.

J_1	$C(3, 6)$	$C(3, 9)$	$C(3, 12)$	$C(3, 15)$
1	-0.0176	-0.1294	-0.0098	0.0917
1.5	-0.1489	-0.004	-0.0051	-0.0018
2	-0.2977	0.111	-0.1028	0.0809
5	-0.426	0.1796	-0.1706	0.1339
40	-0.4559	0.1948	-0.1874	0.1478

effective exchange $J_{\text{eff}} \sim J_2^2/J_1$ between adjacent spin-1/2 at sites $3r$. The system is paramagnetic in the limit of infinite J_1 . The thermodynamic limit at large J_1 is a HAF for localized spins at sites $3r$; the gapless singlet phase has quasi-long-range order.

ED results for $N = 24$ with PBC are entirely consistent with these expectations. Table II lists spin correlation functions at sites $3r$. Spins in different legs have $C(j, k) = 0$ at $J_1 = 0$ and weak correlations at $J_1 = 1$. Near neighbor $C(j, k)$ of the HAF are known analytically³¹ in the thermodynamic limit. $C(3, 9)$ is between third neighbors in a leg where the $J_1 = 0$ result is $C_3 = -0.15074$. Increasing J_1 reverses the signs of $C(j, k)$ in the same leg and makes more negative the $C(j, k)$ in different legs. For $J_1 = 5$ or 40, the $C(j, k)$ in Table II can be compared to the first through fourth neighbors of an 8-site HAF ring: $C(1, 2) = -0.4564$, $C(1, 3) = 0.1958$, $C(1, 4) = -0.1890$ and $C(1, 5) = 0.1491$. The HAF results in the thermodynamic limit³¹ are almost the same at $C_1 = -0.44315$ and $C_2 = 0.18204$. The 8-site correlations are larger as expected than C_3 and $C_4 (= 0.10396)$. The effective Hamiltonian at large J_1 is an HAF with spins at sites $3r$.

The energy gaps Γ_T in Eq. 2 to the lowest triplet and Γ_σ in Eq. 3 to the lowest singlet with reversed inversion symmetry are shown in Fig. 5 as functions of J_1 . The GS is doubly degenerate when $\Gamma_\sigma(J_1) = 0$ at a point or over

an interval. The ladder has $\Gamma_\sigma = 0$ at $J_1 = 1.47$ and 1.58 in Fig. 5. The singlet GS is odd under inversion between these points. The excited states cross at $J_1 = 1.13$ and 2.0 where $\Gamma_T = \Gamma_\sigma$.

The GS degeneracy indicates broken inversion symmetry and a bond-order-wave phase. The BOW phase, either dimer or incommensurate, of the J_1 - J_2 model has recently been studied in detail,¹⁰ and we discuss below the BOW phase of 3/5 ladders. The 5/5 ladder of 24 spins contains 8 unit cells. The 8 spin J_1 - J_2 model has a doubly degenerate GS with $\Gamma_\sigma = 0$ at two values $J_1 > 0$, and $n/4$ degeneracies with $J_1 > 0$ in larger systems. Additional GS degeneracies are likely in longer 5/5 ladders but the larger unit cell poses numerical difficulties. Likewise, the excited state degeneracies $\Gamma_\sigma = \Gamma_T$ at $J_1 = 1.13$ and 2.0 in Fig. 5 give a first estimate of the BOW phase in the thermodynamic limit.

IV. THE 3/5 LADDER

The 3/5 ladder (Fig. 6, inset) has four spins per unit cells and is the first example of a ladder with inequivalent legs. The Hamiltonian is

$$H_{3/5} = J_1 \sum_r \vec{S}_{4r-2} \cdot (\vec{S}_{4r-3} + \vec{S}_{4r-1}) + J_2 \sum_r \vec{S}_r \cdot \vec{S}_{r+2}. \quad (7)$$

There is one rung at each odd-numbered site and two or zero rungs at alternate even-numbered sites. In PBC ladders the sites $4r-2$ and $4r$ are inversion centers at the apices of triangles and pentagons, respectively. Inequivalent legs are additional frustration beyond odd-membered rings and may be responsible for the multiple quantum phases of 3/5 and 5/7 ladders.

The singlet GS of the $N = 24$ PBC system is even under inversion ($\sigma = 1$) up to $J_1 = 1.22$, as shown in Fig. 6, where it becomes odd ($\sigma = -1$) and remains odd until $J_1 = 2.03$ where it switches to $S_G = 1$. The F state of this system has $S_G = 3$, which is reached at $J_1 = 2.30$. Inversion symmetry in the singlet GS is broken at $J_1 = 1.44$ for $N = 16$.

At $J_1 = 1.22$, the GS with $\sigma = \pm 1$ are degenerate (Fig. 6). The plus and minus linear combinations, $|\pm 1\rangle = [|G(\sigma = 1)\rangle \pm |G(\sigma = -1)\rangle] / \sqrt{2}$, are BOWs with broken inversion symmetry and doubled unit cells. The BOW amplitude of the bond between sites j and k is half of the magnitude of the difference $\langle 1|\vec{S}_j \cdot \vec{S}_k|1\rangle - \langle -1|\vec{S}_j \cdot \vec{S}_k|-1\rangle$. This gives

$$B(j, k) = \langle G(\sigma = 1)|\vec{S}_j \cdot \vec{S}_k|G(\sigma = -1)\rangle \quad (8)$$

In general, $B(j, k)$ is finite for sites that are not related by inversion. Since inversion does not interchange the legs, $B(j, k)$ is finite for j and k on different legs, i.e. $j + k$ is an odd integer. For spins in the same leg, some sites are related by inversion and have $B(j, k) = 0$; for example, $B(1, 3) = B(1, 7) = 0$; $B(2, 6) = B(2, 10) = 0$.

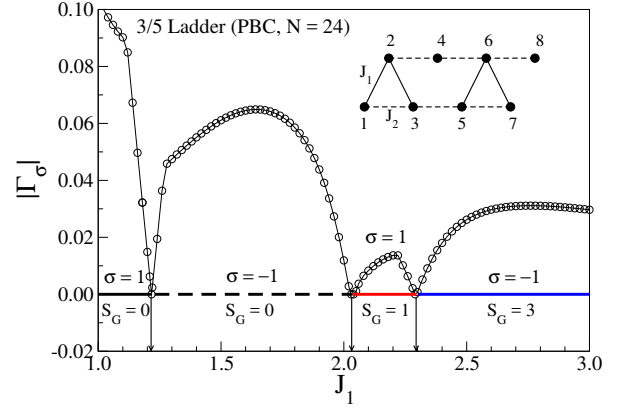


FIG. 6. Excitation Γ_σ in Eq. 3 of the 3/5 ladder with PBC and 24 spins; inset: two unit cells. The quantum phases have spin S_G and inversion symmetry σ .

TABLE III. BOW amplitudes $B(j, k) = -B(j', k') > 0$ in Eq. 8 up to third neighbors in 3/5 ladders with PBC and $J_1 = 1.22$ ($N = 24$) or 1.44 ($N = 16$). Only finite $B(j, k)$ are shown.

j, k	j', k'	$B(j, k)$ $N = 16$	$B(j, k)$ $N = 24$
1, 2	2, 3	0.03992	0.03776
5, 4	4, 3	0.10378	0.06689
2, 4	4, 6	0.22675	0.18063
7, 4	4, 1	0.05334	0.02206
2, 5	3, 6	0.02068	0.02087

Table III lists $B(j, k)$ up to third neighbors for $N = 16$ and 24 spins. The largest amplitude is for first neighbors in the even-numbered leg. The second largest is $B(5, 4) = -B(3, 4)$ at sites without a J_1 rung; $B(1, 2) = -B(2, 3)$ at sites connected by J_1 is smaller but decreases more slowly with system size.

Next we consider 3/5 ladders at large J_1 . For 24 spins, we find $S_G(J_1, N) = 3$ from $J_1 = 2.30$ in Fig. 6 to $J_1 = 6.87$ in Fig. 7, where the GS reverts to $S_G = 0$. The GS of the 16 spin system is $S_G = 2$ over almost exactly the same J_1 range. The F phase with an unpaired spin per triangle is limited to intermediate J_1 . We are not aware of another spin-1/2 chain with an intermediate F phase between two AF phases.

Selected spin correlation functions $C(j, k)$ of 3/5 ladders are listed in Table IV. PBC ladders have two different first neighbor correlations and three different second neighbor correlations. The J_1 dependencies follow the discussion above of 3/4 ladders, especially with respect to triangles, and the $J_1 = 0$ systems are of course identical. $C(1, 3)$ changes sign around $J_1 \sim 2$ and is close to 0.25 by $J_1 = 10$, where $C(1, 2) = C(2, 3)$ is close to -0.50 . The effective AF exchange between spins 3 and 5 in adjacent triangles is $\rho_b^2 = 4/9$ in the limit $J_1 \gg 1$; $C(3, 5)$ approaches a finite constant at $J_1 > 40$.

The GS of triangles is a doublet at large J_1 when other degrees of freedom are frozen out. The 3/4 ladder reduces

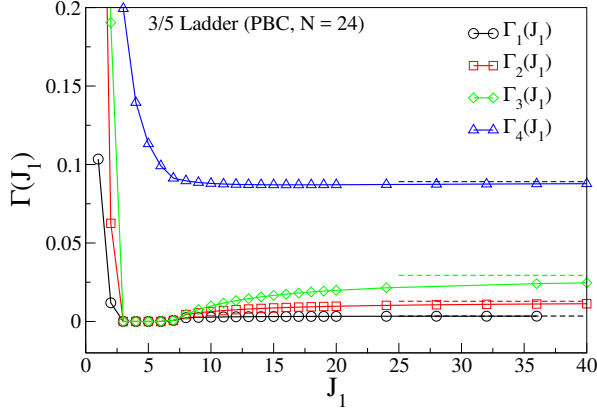


FIG. 7. Excitation Γ_S in Eq. 2 of a 3/5 ladder with PBC and 24 spins; the GS is a singlet for $J_1 > 6.87$. The dashed lines are the $J_1 \rightarrow \infty$ excitations of $H_{\text{eff}}(24)$ in Eq. 9.

TABLE IV. First and second neighbor spin correlation functions $C(j, k)$ of the 3/5 ladder with PBC and $N = 24$ spins.

J_1	$C(1, 2),$ $C(2, 3)$	$C(3, 4),$ $C(4, 5)$	$C(1, 3)$	$C(3, 5)$	$C(2, 4),$ $C(4, 6)$
0	0	0	-0.4489	-0.4489	-0.4489
1	-0.0795	-0.0032	-0.2709	-0.5758	-0.4255
1.5	-0.2221	0.0041	-0.1394	-0.5218	-0.3430
2	-0.2983	0.0185	-0.0399	-0.4484	-0.2950
2.5	-0.4534	0.0676	0.2078	-0.3314	-0.1443
5	-0.4900	0.0583	0.2431	-0.2553	-0.0795
10	-0.4978	0.0508	0.2486	-0.2215	-0.0472
20	-0.4995	0.0456	0.2497	-0.2062	-0.0335
40	-0.4999	0.0428	0.2499	-0.1985	-0.0267

to F exchange between adjacent triangles. The 3/5 ladder in this limit has AF exchange $j_2 = 4/9$ between the bases of adjacent triangles and F exchange $j_1 = -1/3$ between apices (sites $4r - 2$) and spins at sites $4r$. A 3/5 ladder of $N = 4n$ spins reduces to a PBC system of $N/2$ spins with an effective Hamiltonian that becomes exact as $J_1 \rightarrow \infty$.

$$H_{\text{eff}}(N) = j_1 \sum_{r=1}^{N/2} \vec{S}_{2r} \cdot \vec{S}_{2r+2} + j_2 \sum_{r=1}^{N/4} \vec{S}_{4r-2} \cdot \vec{S}_{4r+2} \quad (9)$$

Eq. 9 is defined on the even-numbered leg with exchange j_1 between first neighbors and j_2 between sites that correspond to adjacent triangles. When $j_2 > 0$, H_{eff} is a frustrated spin chain for either sign of j_1 . If we set $j_1 = 0$, the first neighbor spin correlations in the j_2 chain is $C(3, 5) = (1 - 4 \ln 2)/9 = -0.19695$, which is close to the $N = 24$, $J_1 = 40$ entry in Table IV. The dashed lines Fig. 7 are excitations of $H_{\text{eff}}(24)$ with $j_1 = -1/3$ and $j_2 = 4/9$. The six spins at sites $4r$ are weakly coupled and frustrated; they account for small gaps up to Γ_3 . The same reasoning explains why $H_{\text{eff}}(16)$ has small gaps Γ_1 , Γ_2 and a larger gap Γ_3 . The effective Hamiltonian returns equally quantitative excitations for $N = 12$, 16 and 20 spins.

TABLE V. Spin correlation functions $C(j, k)$ at sites 3, 7, 11, 15 of the 5/7 ladder with PBC and $N = 24$. Refer to Fig. 8, inset, for site numbers.

J_1	$C(3, 7)$	$C(3, 11)$	$C(3, 15)$
1	0.1807	0.1161	0.0974
1.8	0.1734	-0.1102	-0.1747
5	0.2435	0.2372	0.2389
40	0.2499	0.2498	0.2498

H_{eff} has been discussed previously by Hamada et al.³² in the context of a frustrated spin chain related to the J_1 - J_2 model. The GS with $j_2 > 0$ is F for $j_1 \leq -2j_2$ and a singlet otherwise.³² The thermodynamic limit for $j_1/j_2 = -3/4$ is a gapless AF phase with a non-degenerate singlet GS and quasi-long-range spin correlations.

V. THE 5/7 LADDER

The 5/7 ladder (Fig. 1a) has eight spins per unit cell and two J_1 rungs per eight exchanges $J_2 = 1$. The Hamiltonian is

$$H_{5/7} = J_1 \sum_r \left(\vec{S}_{8r-4} \cdot \vec{S}_{8r-3} + \vec{S}_{8r+1} \cdot \vec{S}_{8r+2} \right) + J_2 \sum_r \vec{S}_r \cdot \vec{S}_{r+2}. \quad (10)$$

The legs are not equivalent. PBC ladders have inversion centers at every other site (3, 7, 11, ...) of the odd-numbered leg, and the unpaired spins at large J_1 are at these sites. Second order perturbation theory returns a F effective exchange $J_{\text{eff}} \sim -J_2^2/J_1$ between the unpaired spins that are adjacent to the same end of a J_1 rung. The ladder has a F phase at large but finite J_1 , albeit with small J_{eff} . In 5/5 ladders with $J_{\text{eff}} > 0$, the unpaired spins are next to the opposite ends of a J_1 rung.

ED results for the PBC ladder of $N = 24$ spins are shown in Table V and Fig. 8. The sites are second, fourth and sixth neighbors in a leg. The $J_1 = 1$ spin correlations are close to the available thermodynamic results at $J_1 = 0$: $C_2 = 0.1820$ and $C_4 = 0.1040$. The GS is in the singlet sector at $J_1 = 1$ or 1.8 and in the $S_G = 3$ sector at $J_1 = 5$ or 40. The signs of $C(3, 11)$ and $C(3, 15)$ are reversed at $J_1 = 1.8$. All the correlations approach 0.250 at large J_1 as expected for an HAF with F exchange and spins at every fourth site.

As seen in Fig. 8, the singlet GS is even under inversion ($\sigma = 1$) up to $J_1 = 1.43$, where it is degenerate with $\sigma = -1$, and it remains in the $\sigma = -1$ sector up to $J_1 = 1.76$. Then the singlet GS is doubly degenerate with $\sigma = \pm 1$ up to 1.87. The GS between 1.87 and 2.18 is a non-degenerate triplet in the $S_G = 1$, $\sigma = -1$ sector and a degenerate triplet from 2.18 to 2.35 with $\sigma = \pm 1$. The GS switches to $S_G = 3$ at $J_1 = 2.35$ at the onset of the F phase for three unit cells. The F phase of the $N = 16$ ladder and four unpaired spins is reached

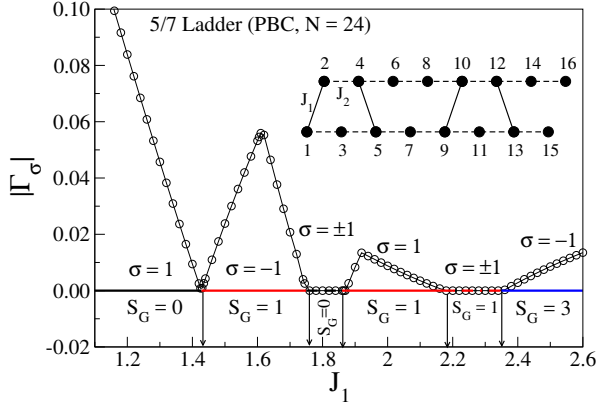


FIG. 8. Excitation Γ_σ in Eq. 3 of a 5/7 ladder with PBC and 24 spins; inset: two unit cells. The quantum phases have spin S_G and inversion symmetry σ .

at the same J_1 . DMRG results for longer OBC ladders of $N = 8n + 2 = 50$ or 100 spins confirm a F phase with $S_G = n$ for $J_1 > 2.35$ and $S_G/N = 0.125$ in the thermodynamic limit.

We return below to the multiple GS of small 5/7 ladders after reporting DMRG results for longer ladders. The F limit of one unpaired spin per ring is also reached at $J_1 = 2.35$ in long ladders with OBC as shown by the dashed line in Fig. 9. The DMRG results for $S_G(J_1, N)$ vs. N for smaller J_1 are reasonably linear in Fig. 9 and increase considerably more slowly. The location of $\Delta S_G(J_1, N) = 1$ steps is limited by the numerical accuracy of the total energy and minimally requires one unit cell, $\Delta N = 8$. Integer S_G leads to constant plateaus over intervals in N , as shown best at $J_1 = 1$ where $S_G(1, N) = 5$ is reached around $N = 470$. There is roughly one unpaired spin per 12 rings (6 unit cells). ED for $N = 18$ or 26 indicates that the spins are delocalized at $J_1 = 1$ and cannot be rationalized by qualitative arguments. Aside from $S_G(1, N) = 1$ around $N = 54 \pm 4$, the $J_1 = 1$ plateaus in Fig. 9 have approximately equal widths implying $S_G \propto N$ that is consistent with a conjectured F phase in the thermodynamic limit. It is weak ferromagnetism at best, and longer ladders will be needed to verify the conjecture. The proportionality of $S_G(J_1, N)$ to system size is better realized at $J_1 = 1.3$ or 1.5 in ladders with a F phase.

We anticipated that $S_G(J_1, N)$ would increase faster with system size on increasing J_1 from 1.5 to 2.35, where the limit $S_G = n$ of one spin per ring is reached. That is not the case, however. The DMRG results in Fig. 10 show that the GS of the OBC ladder of $N = 98$ spins (24 rings) has $S_G = 0$ up to $J_1 = 0.85$, $S_G = 1$ from 0.85 to 1.23, $S_G = 2$ from 1.23 to 1.43, $S_G = 3$ from 1.43 to 1.60, and $S_G = 4$ from 1.60 to 1.75. The GS is again a singlet, $S_G = 0$, in the range $1.75 < J_1 < 2.18$. Almost exactly the same $S_G = 0$ range is obtained for an OBC ladder of 50 spins, while the $S_G = 0$ range for the PBC ladder of 24 spins in Fig. 8 is limited to

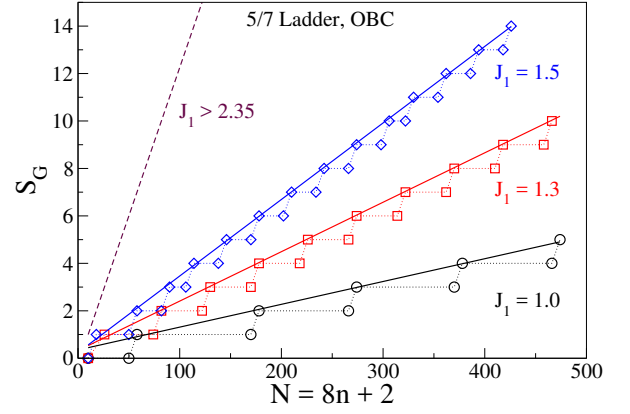


FIG. 9. DMRG results for the size dependence of the ground-state spin $S_G(J_1, N)$ in 5/7 ladders with the indicated J_1 . The dashed line is the F limit for $J_1 > 2.35$. The marked points correspond to system sizes at the edges of the plateaus are shown.

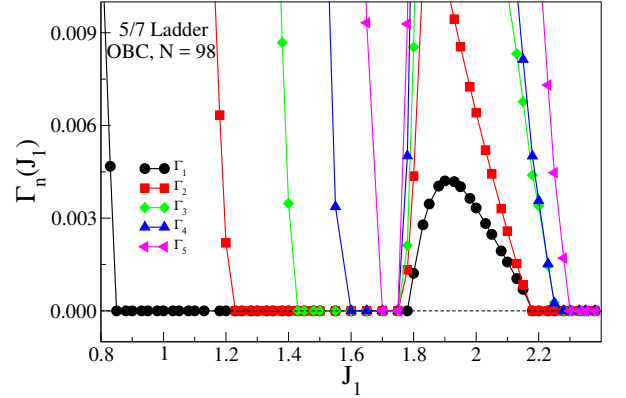


FIG. 10. DMRG results for the GS spin $S_G(J_1, N)$ of a 5/7 ladder of $N = 98$ spins and OBC as a function of J_1 . The AF phase with $S_G = 0$ is regained between $J_1 = 1.75$ and 2.18.

$1.75 < J_1 < 1.87$, beyond which we have $S_G = 1$ up to $J_1 = 2.35$. The longer ladders do not have a triplet GS in this range. Increasing J_1 leads to a remarkable reentrant AF phase at intermediate $1.75 < J_1 < 2.18$. We do not understand how frustrated exchange and inequivalent legs in 5/7 ladders return a singlet GS at intermediate J_1 .

The triplet GS in Fig. 8 is doubly degenerate ($\sigma = \pm 1$) in the J_1 interval 2.18 to 2.35. Finite 5/7 ladders with PBC and $N = 16$ or 24 spins have broken vector chiral symmetry in this range. The degeneracy is between $S^z = 1, \sigma = 1$ and $S^z = -1, \sigma = -1$. The spin current at sites j, k is the matrix element $\pm \kappa(k, j)$

$$\begin{aligned} \kappa_z(j, k) &= \langle \Psi_G(-) | \vec{S}_j \times \vec{S}_k | \Psi_G(+) \rangle \\ &= \frac{i}{2} \langle \Psi_G(-) | (S_j^+ S_k^- - S_j^- S_k^+) | \Psi_G(+) \rangle, \end{aligned} \quad (11)$$

where $|\Psi_G(\pm)\rangle = |G(S^z = \sigma = \pm 1)\rangle$.

The arrows in Fig. 1(a) indicate the direction of spin currents. In finite regular chains, spin currents are absent

for purely isotropic exchange without an applied magnetic field. Either anisotropic exchange⁹ or an applied field³³ is typically required for broken vector chiral symmetry in these systems. However, we find that skewed ladders lead to nonzero spin currents even for isotropic exchange in the absence of applied magnetic field.

VI. DISCUSSION AND SUMMARY

We have obtained the quantum phases of frustrated 2-leg ladders with skewed rungs and found both F and AF phases at large J_1/J_2 when an unpaired spin is localized on every odd-membered ring. Perturbation calculations on odd ringed ladders give a simple pattern of effective exchanges J_{eff} between unpaired spins. Delocalization within 3-membered rings leads to first-order corrections with $J_{\text{eff}} \propto J_2$ between sites with finite spin density. The 3/4 ladder is F with $J_{\text{eff}} < 0$ while the 3/5 ladder is AF with frustrated $j_1 < 0$ and $j_2 > 0$ in Eq. 9.

The unpaired spin at large J_1/J_2 is localized at one site in 5 and 7-membered rings with $J_{\text{eff}} \propto J_2^2/J_1$. The unpaired spin in larger rings is delocalized over an odd number of sites, three sites for 9 or 11-membered rings. The unpaired spins of the 5/5 or 7/7 are on opposite sides of a J_1 rung with $J_{\text{eff}} > 0$. They are on the same side (in the same leg) in the 5/7 ladder with $J_{\text{eff}} < 0$. The 5/7 and 3/4/5/4 ladders have 8 spins per unit cell and are F and AF respectively at large J_1 , while the 7/7 and 5/4 ladders with 5 spin per unit cell are AF and F. Unpaired spins on opposite sides of a J_1 rung have $J_{\text{eff}} > 0$ but a second J_1 rung in a 4-membered ring changes the sign to $J_{\text{eff}} < 0$. The same result holds for unpaired spins in the same leg: $J_{\text{eff}} < 0$ when separated by a J_1 rung, $J_{\text{eff}} > 0$ when separated by two rungs.

2-leg ladders with skewed rungs have inversion symmetry at some sites, rather than at all sites in the J_1 - J_2 model, the 3/3 ladder. It is therefore not surprising to find BOW phases with $S_G = 0$ in the 5/5 or 3/5 ladder

around $J_1 \sim J_2$. The BOW amplitudes are more complicated than the dimer phase of the J_1 - J_2 model because the unit cells contain several spins instead of just one. Longer 5/5 or 3/5 ladders with PBC than considered here may also support incommensurate phases.

At intermediate J_1/J_2 , the 3/5 and 5/7 ladders have magnetic phases with $S_G > 0$ but considerably less than one unpaired spin per ring. The 3/5 ladder is AF for both small and large J_1 but is magnetic at intermediate J_1 from about 2.3 to 6.9. The 5/7 ladder is F with an unpaired spin per ring for $J_1 > 2.3$, weakly F for $J_1 = 1$ to 1.6, and quite remarkably AF between $J_1 \sim 1.75$ and 2.17. Both ladders have inequivalent legs in addition to odd-membered rings. The evolution of S_G with J_1 is not monotonic in either ladder. As for the 5/7 ladder with $J_1 = J_2$, the DMRG result in Fig. 9 is consistent with $S_G \propto N$ and suggests weak ferromagnetism that remains to be confirmed in considerably longer ladders.

A novel feature of 2-leg spin ladders with skewed legs is that both small and large J_1 correspond to extended systems, two HAFs when $J_1 = 0$ and a Heisenberg chain with J_{eff} of either sign for spins localized on odd-membered rings when $J_1 \gg J_2$. The conventional 2-leg ladder, $H_{4/4}$, has localized singlets at rungs when $J_1 \gg J_2$ and a continuous evolution with J_1 from gapless HAFs on legs to localized rungs. The evolution of $S_G(J_1)$ of ladders with skewed rungs is more complex and includes magnetic phases at intermediate J_1 before reaching an AF or F phase according to the pattern of J_1 rungs.

ACKNOWLEDGMENTS

MK thanks DST for Ramanujan fellowship and computation facility provided under the DST project SNB/MK/14-15/137. SR thanks DST for funding this work under various programs.

* First and second authors have contributed equally ;
geetgiri1@gmail.com

† dayasindhu.dey@bose.res.in

‡ manoranjan.kumar@bose.res.in

§ ramasesh@sscu.iisc.ernet.in

¶ soos@princeton.edu

¹ H. Bethe, *Z. Phys.* **71**, 205 (1931).

² L. Hulthén, *Ark. Mat. Astron. Fys.* **26**, 106 (1938).

³ F. D. M. Haldane, *Phys. Lett.* **93A**, 464 (1983).

⁴ R. Chitra, S. Pati, H. R. Krishnamurthy, D. Sen, and S. Ramasesha, *Phys. Rev. B* **52**, 6581 (1995); S. Sahoo, V. D. P. Goli, D. Sen, and S. Ramasesha, *J. Phys.: Condens. Matter* **26**, 276002 (2014).

⁵ C. K. Majumdar and D. K. Ghosh, *J. Math. Phys.* **10**, 1399 (1969).

⁶ P. Lecheminant, *Frustrated Spin Systems*, edited by H. T. Diep (World Scientific, Singapore, 2004) Chap. 6, p. 307.

⁷ M. Hase, H. Kuroe, K. Ozawa, O. Suzuki, H. Kitazawa, G. Kido, and T. Sekine, *Phys. Rev. B* **70**, 104426 (2004).

⁸ J. Sudan, A. Lüscher, and A. M. Läuchli, *Phys. Rev. B* **80**, 140402 (2009); D. V. Dmitriev and V. Y. Krivnov, *Phys. Rev. B* **77**, 024401 (2008).

⁹ S. Furukawa, M. Sato, S. Onoda, and A. Furusaki, *Phys. Rev. B* **86**, 094417 (2012).

¹⁰ Z. G. Soos, A. Parvej, and M. Kumar, *J. Phys.: Condens. Matter* **28**, 175603 (2016).

¹¹ A. W. Sandvik, *AIP Conf. Proc.* **1297**, 135 (2010).

¹² M. B. Smith and J. Michl, *Chem. Rev.* **110**, 6891.

¹³ S. Prodhon and S. Ramasesha, *arXiv:1610.00562*.

¹⁴ S. Thomas, S. Ramasesha, K. Hallberg, and D. Garcia, *Phys. Rev. B* **86**, 180403 (2012).

¹⁵ S. W. Cheong and M. Mostovoy, *Nature Mat.* **6**, 13 (2007).

¹⁶ H. Katsura, N. Nagaosa, and A. V. Balatsky, *Phys. Rev. Lett.* **95**, 057205 (2005).

- ¹⁷ S. Ren and M. Wuttig, [Adv. Mater.](#) **24**, 724 (2012).
- ¹⁸ K. Kobayashi, S. Horiuchi, R. Kumai, F. Kagawa, Y. Murakami, and Y. Tokura, [Phys. Rev. Lett.](#) **108**, 237601 (2012).
- ¹⁹ T. Barnes, E. Dagotto, J. Riera, and E. S. Swanson, [Phys. Rev. B](#) **47**, 3196 (1993).
- ²⁰ M. Azzouz, L. Chen, and S. Moukouri, [Phys. Rev. B](#) **50**, 6233 (1994).
- ²¹ S. R. White, [Phys. Rev. Lett.](#) **69**, 2863 (1992); [Phys. Rev. B](#) **48**, 10345 (1993).
- ²² U. Schollwöck, [Rev. Mod. Phys.](#) **77**, 259 (2005).
- ²³ K. A. Hallberg, [Advances in Physics](#) **55**, 477 (2006).
- ²⁴ M. Kumar, Z. G. Soos, D. Sen, and S. Ramasesha, [Phys. Rev. B](#) **81**, 104406 (2010).
- ²⁵ D. Dey, D. Maiti, and M. Kumar, [Papers in Physics](#) **8** (2016).
- ²⁶ S. Ramasesha and Z. G. Soos, [J. Chem. Phys.](#) **80**, 3278 (1984).
- ²⁷ Z. G. Soos and S. Ramasesha, *Valence Bond Theory and Chemical Structure*, edited by D. J. Klein and N. Trinajstić (Elsevier, Amsterdam, 1989) p. 81.
- ²⁸ H. M. McConnell, [J. Chem. Phys.](#) **39**, 1910 (1963).
- ²⁹ C. Kollmar and O. Kahn, [Acc. Chem. Res.](#) **26**, 259 (1993).
- ³⁰ A. Izuoka, S. Murata, T. Sugawara, and H. Iwamura, [J. Am. Chem. Soc.](#) **109**, 2631 (1987).
- ³¹ M. Shiroishi and M. Takahashi, [J. Phys. Soc. Jpn.](#) **74**, 47 (2005).
- ³² H. Takehiko, K. Jun-ichi, N. Shin-ichi, and N. Yuhei, [J. Phys. Soc. Japan](#) **57**, 1891 (1988).
- ³³ T. Hikihara, L. Kecke, T. Momoi, and A. Furusaki, [Phys. Rev. B](#) **78**, 144404 (2008).